

Evaporation Kinetics and Breaking of a Thin Water Liquid Bridge between Two Plates of Silicon Wafer

Etienne Portuguez, Arnaud Alzina, Philippe Michaud, Agnès Smith*

Université de Limoges, Limoges, France

Email: *agnes.smith@unilim.fr

Received 25 May 2016; accepted 27 June 2016; published 30 June 2016

Copyright © 2016 by authors and Scientific Research Publishing Inc.

This work is licensed under the Creative Commons Attribution International License (CC BY).

<http://creativecommons.org/licenses/by/4.0/>



Open Access

Abstract

In ceramic processing, the study of the different phases of the drying stage considers the material at a macroscopic scale. Very often, the various parameters (among which the temperature and the relative humidity) are chosen in an empirical way, mostly through visual observations. This stage is governed by capillary phenomena which take place within the material, responsible for both the shrinkage and the risk of cracks which can damage the final piece. As part of a better understanding of the local mechanisms during drying, liquids contained in the pores have been reproduced in an ideal case. Drying kinetics and parameter measurements from 303 to 343 K of deionized water liquid bridges between two plates of silicon wafers are presented. Experimental work was carried out using specific device to create liquid bridges, coupled with image analysis and within an adapted instrumented climatic chamber. While the volume and the exchange surface of liquid bridges decrease regularly throughout the drying process, contact angles only diminish at the end. One of the four contact angles may have a different variation, which results in a pinned contact line in its area and reveals a local change of the surface state. From these measurements and observations, the liquid bridge break is proposed as a cracking criterion of porous materials during drying. Indeed, the challenge is to limit the risk of cracking and damaging pieces during this crucial step in material processing.

Keywords

Liquid Bridge, Volume, Contact Angle, Evaporation, Drying

*Corresponding author.

1. Introduction

The creation of ceramic materials is generally divided into a set of common steps [1]. Initially, raw materials are prepared and mixed with additives and possibly a solvent to give either a dry (or semi-dry) powder, a plastic paste or a suspension. Then, the mixture is shaped. Except in the case of dry shaping processes such as pressing, a drying step is necessary to remove the liquid phase before the firing stage, which gives to the material its final characteristics. These considerations are presented in **Figure 1**. Drying is an energy-consuming but also a delicate stage as the shrinkage and the possible cracks determine the strength and the quality of the final piece. The different steps of the drying stage have been studied in detail throughout the 20th century [2]. However, the methods used do not provide any indications concerning the drying behavior at a local scale as they consider the system on a macroscopic scale: whether it is experimental approaches (for instance the Bigot curves [3], where the sample mass loss is plotted as a function of its linear shrinkage) or numerical resolutions (for example the Darcy's law [4], which describes the flow of an incompressible fluid through a porous medium). Here, we investigate the case of drying materials by evaporation under various temperatures and relative humidities of the drying air, in particular the local capillary phenomena during the departure of the liquid phase. During drying, the material passes, at a local scale, from an almost liquid-saturated condition to a state where shrinking liquid bridges are surrounded by a binary mix of air and liquid vapor [5]. At a local scale, the liquid volumes and pore sizes are small enough to consider that gravity effects are negligible compared to the other forces, namely the capillary forces directly related to the hydrostatic pressure and surface tension of the liquid bridges [6] [7].

Recent studies described the evolution of surface tension not only as a function of temperature but also as a function of relative humidity [8] [9]. This article provides new local data about the behavior of liquid bridges in a confined geometry. Such data aim at a better understanding of the drying stage when water is confined in pores. They can also be useful to provide data in order to create an accurate numerical model based on representative experimental values of the pore sizes mechanisms. To the best knowledge of the authors, neither the experimental setup developed for this study nor the kinetic data recorded during drying under different temperature and humidity conditions of water meniscus squeezed between two plates have been reported in the literature.

2. Materials and Methods

2.1. Climatic Chamber

Measurements of the characteristics of the menisci are made at a given temperature and relative humidity. An

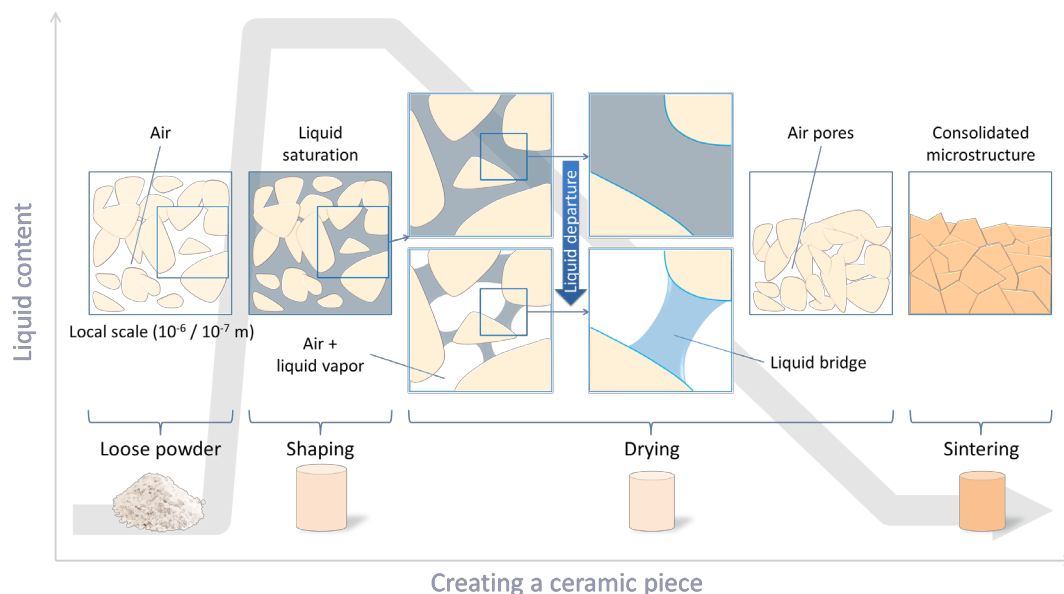


Figure 1. Evolution of the microstructure throughout the creation of a ceramic piece.

environmental chamber as shown in **Figure 2** was used to set the temperature and the relative humidity of the drying air. The temperature is adjusted by armored heaters, associated with the chamber controller with an accuracy of 0.1 K. Air humidity is provided by a boiler. Platinum psychrometric sensors control the humidity of air with an accuracy of 0.1%. If the relative humidity is higher than the set point, it is stabilized using a cooling unit linked to the chamber. The environmental chamber is computer controlled and data can be checked in real time. The climatic chamber has a zero diopter glass door to directly observe the liquid bridge during the drying stage. As it was not possible to put a collimated light source into the chamber given the harsh conditions, a white background has been added to the system and a white led diffuses light to obtain a sufficient contrast to observe the liquid. The system of the climatic chamber is limited at low (~ 283 K) and high (~ 353 K) temperatures. Indeed, it is difficult to reach low relative humidity levels at low temperatures, and at high temperatures the cooling unit laboriously reaches the highest relative humidity levels. Therefore, results that are presented in this paper are limited to temperatures between 303 and 343 K and relative humidities from 20% to 100%.

To avoid any temperature gradient, before creating a liquid bridge, the liquid is placed inside the climatic chamber so that it is at the same temperature as the target temperature. The liquid bridge creation is detailed in the following section.

2.2. Liquid Bridges Creation

A specific module has been created in order to mimic the conditions of a liquid bridge within a porous material. It was then placed within the climatic chamber to observe drying liquid bridges. A detailed view of the liquid bridges creation module is presented in **Figure 3**. It is made of a rotating movable part attached to a fixed frame. Thus, the movable part can make a vertical translation using a $20 \text{ mm} \pm 1 \mu\text{m}$ of travel micrometer, and a rotation with an accuracy of 0.1° along an axis perpendicular to that of the translation. Two substrates are required to make a measurement. They are beforehand cleaned with ultrasound in an acetone bath and the surface is then washed with ethanol before being dried. The substrates are fixed on the system and their parallelism is checked using the optical camera. In order to measure the characteristics of deionized water menisci, a drop is produced at the end of a capillary tube and elongated by gravity. Then, they are separated from one another of about 1.5 cm so a pendant drop can be slowly deposited on the lower substrate. Finally, the upper substrate is moved toward the drop and the liquid bridge is created. According to the distance between the two substrates, which can be in this study 0.25, 0.5 or 1 mm, the typical volumes of the deposited droplets are 1, 5 or $10 \mu\text{L}$. An Eppendorf Multipette[®] plus allowed to create pendant drops with such initial volumes with a precision of 1%. Deionized

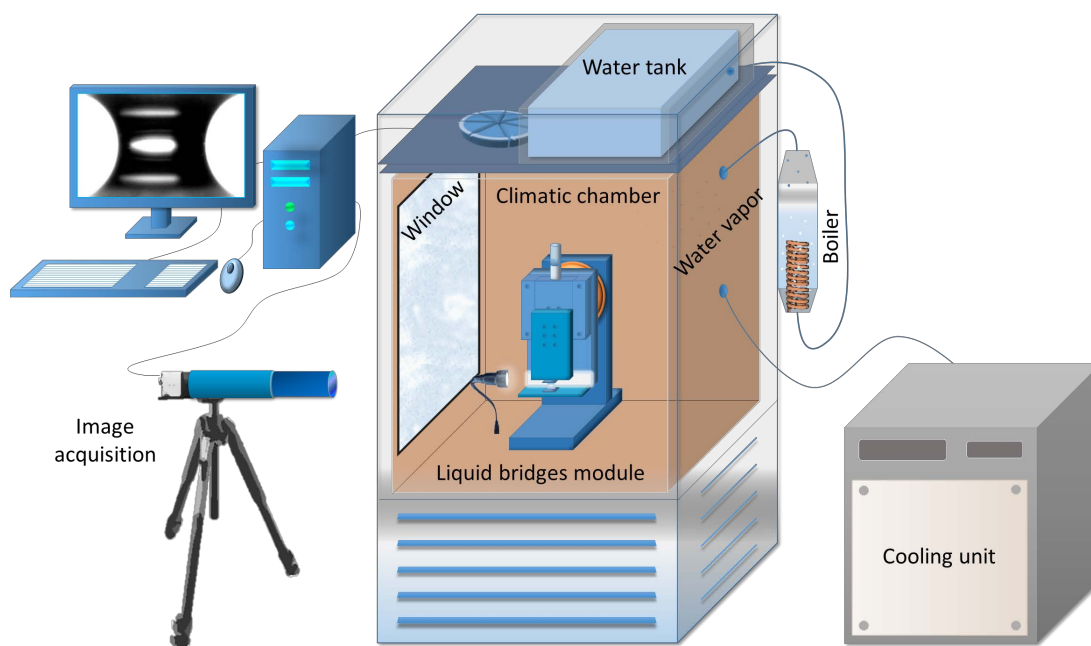


Figure 2. Experimental device for the observation of liquid bridges.

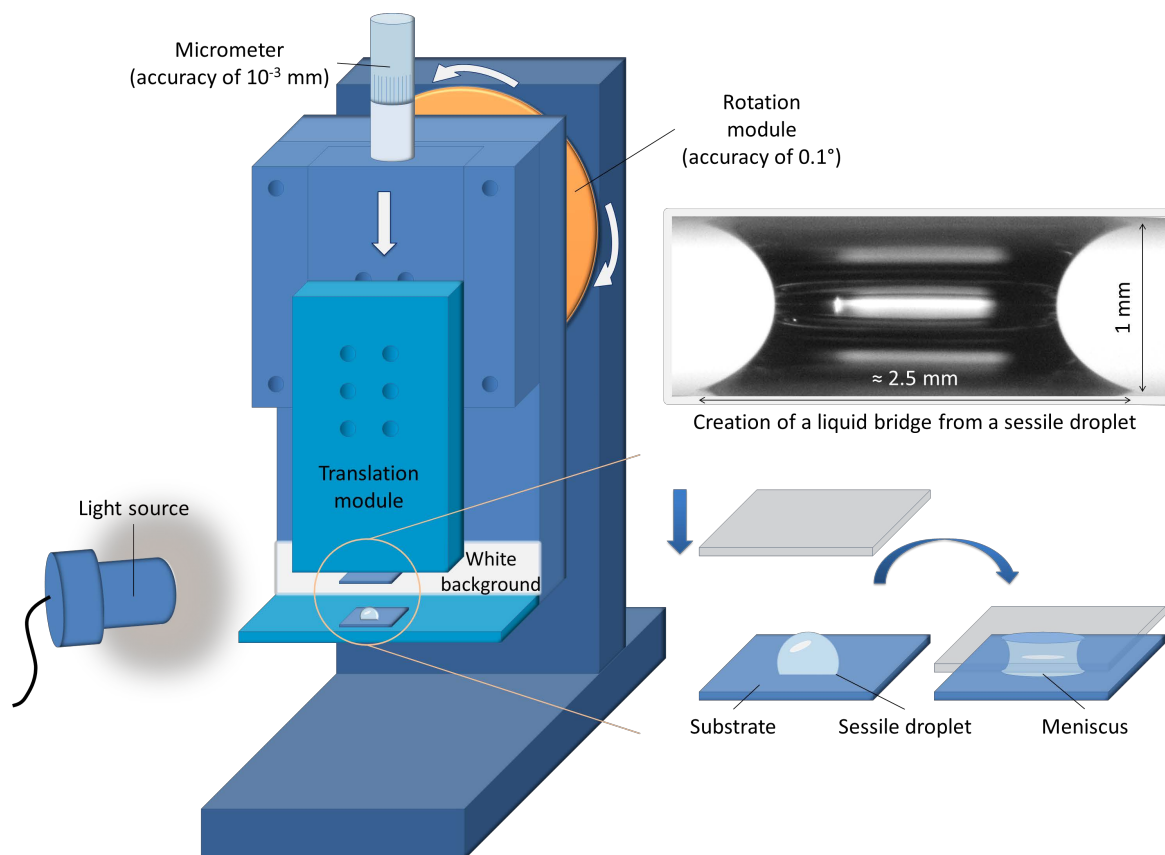


Figure 3. Schematic representation of the liquid bridges module used to create menisci.

water (conductivity $< 1 \text{ mS}\cdot\text{m}^{-1}$) was used for drops and for the water tank providing humidity into the climatic chamber, thus the studied liquid and surrounding vapor have the same composition. Water density is of $1.000 \pm 0.005 \text{ g}\cdot\text{mL}^{-1}$ at 293 K and for the presented work it can decrease to $0.977 \pm 0.005 \text{ g}\cdot\text{mL}^{-1}$ at 343 K.

2.3. Image Acquisition

In order to obtain suitable images of the liquid bridge at regular time intervals, a monochrome camera with charge-coupled device (CCD) was used, model UI-148SE-M from manufacturer IDS Imaging. The camera has a 5 M pixel 1/2" sensor, a resolution of 2560×1920 pixels and a rate of $6 \text{ images}\cdot\text{s}^{-1}$. It was coupled with an optical QIOPTIC which is made of two components, one model 35-08-06-000 and one model 35-00-03-000 which gives with a QIOPTIC 12.5:1 zoom an optical of 100 mm/0.062 1/2".

The breaking of the liquid bridge and the resulting particular geometries were observed using a fast camera. This camera is a Photron FASTCAM 1024 PCI with a $17.4 \text{ mm} \times 17.4 \text{ mm}$ color sensor. Each pixel measures $17 \mu\text{m} \times 17 \mu\text{m}$. The maximum frame rate at full resolution 1024×1024 is $1000 \text{ images}\cdot\text{s}^{-1}$. The resolution may be lowered to obtain higher frame rate up to $109,500 \text{ images}\cdot\text{s}^{-1}$ when the resolution is 128×16 .

2.4. Liquid Bridge Volume and Area Evaluation

The present study also proposes an evaluation of the volume and the area of the liquid bridge during drying. Image analysis was used to realize these measurements, and consisted in a three steps procedure. First, liquid bridges with an initial volume of $1.0, 5.0$ or $10.0 \mu\text{L} \pm 0.1 \mu\text{L}$ were produced and observed during drying. The millimetric dimensions of the liquid bridges are given in **Figure 4(a)**. Images were taken each minute and with a narrower interval of time at the end of drying. After the image acquisition step, pictures were cropped in order to retain the liquid part and remove the image of the two substrates. As the pictures were given in grayscale, a threshold allowed to detect the edge of the liquid bridge (**Figure 4(b)**). Using the distance between the two sub-

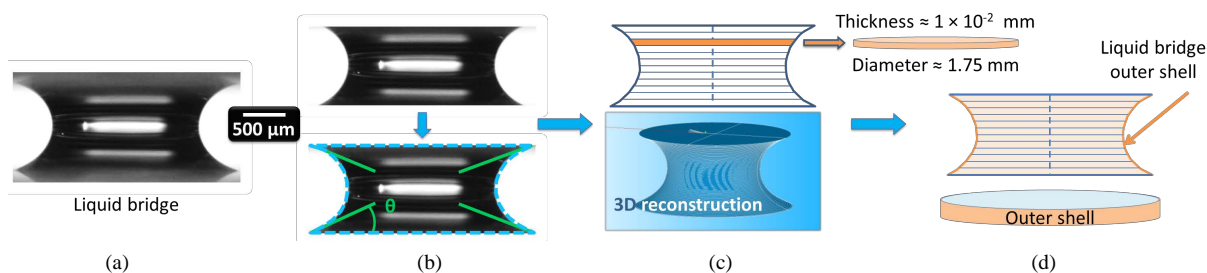


Figure 4. Water liquid bridge volume and area evaluation: (a) liquid bridge of deionized water; (b) cropped image of the liquid bridge followed by edge detection (dashed line) and evaluation of the four contact angles; (c) liquid bridge volume evaluation (gravity center in dashed line) and three-dimensional reconstruction; (d) liquid bridge outer shell evaluation (exchange surface).

strates as a standard to convert pixels values in meters, namely 0.25, 0.5 or 1 mm, a computer program was developed in the laboratory to evaluate the volume and the area of the liquid bridge. More precisely, the liquid bridge was divided into subsections and a circular revolution allowed the evaluation of all the subvolumes. The volume then resulted from their addition.

This method not only provided an accurate evaluation of the liquid bridge volume but also allowed to locate precisely the gravity center of each subvolume, which minimized the effect of any shift due to additional micro-vibrations in the system associated to the convection within the climatic chamber. The liquid bridge was then rebuilt in three dimensions (Figure 4(c)). To evaluate the exchange surface, only the outer shell was retained. Moreover, the surfaces in contact with the substrates were not considered in this evaluation (Figure 4(d)).

Liquid bridges are observed until they break, which corresponds to the final stage of the drying of porous materials when water confined between two neighboring particles evaporates as illustrated in Figure 5. A comprehensive study of the evaporation of liquid bridges between two glass spheres has recently been proposed [10]. However, relative humidity and temperature were respectively fixed at 25% and 294 K.

The presented equipment and numerical tools enabled to carry out a set of measurements at different temperatures and relative humidities.

3. Results and Discussion

3.1. Liquid Bridge Volume and Exchange Surface Evolution

Liquid bridges have been created between two plates of silicon wafer. By creating a sessile drop on a silicon wafer, the observed contact angles are less than 50° which is a case of wettability. Of course, in reality and in porous materials, surfaces are never perfectly flat and the study of real solid surfaces nowadays becomes a major issue [11]. Nevertheless, our experimental approach with silicon wafers in an ideal case provides a first idea of the evolution of the different geometrical parameters of liquid bridges (Figure 6).

The liquid bridges height used in this study and the corresponding liquid volumes are given in the Table 1.

The results for these different heights and volumes are given in Figure 7. As a first observation, it appears that the volume and surface evolutions as a function of time have similar behavior, whatever the height of the liquid bridge and the starting volume are. Indeed, the volume curves have a convex shape as a function of time and the rate of volume loss decreases as the drying evolves. This is directly connected to change of shape where the most significant geometry changes occur at the neck of the liquid bridges at the end of the drying process. Regarding the exchange surface curves, they all present a concave shape. However, due to the contact with the two substrates, the initial surfaces are less than the surface of a spherical water drop with the same initial volume. For information, the initial surface of a perfect spherical drop of $8 \mu\text{L}$ is 19.34 mm^2 , while here in the case of a 1 mm height liquid bridge with an initial volume of $8 \mu\text{L}$, the exchange surface with the drying air is about 12 mm^2 , whatever the temperature is.

3.2. Contact Angle Evolution

From image acquisition, the four contact angles of each observed liquid bridge have been evaluated by image analysis. The results obtained with a liquid bridge height of 0.5 mm are presented in Figure 8.

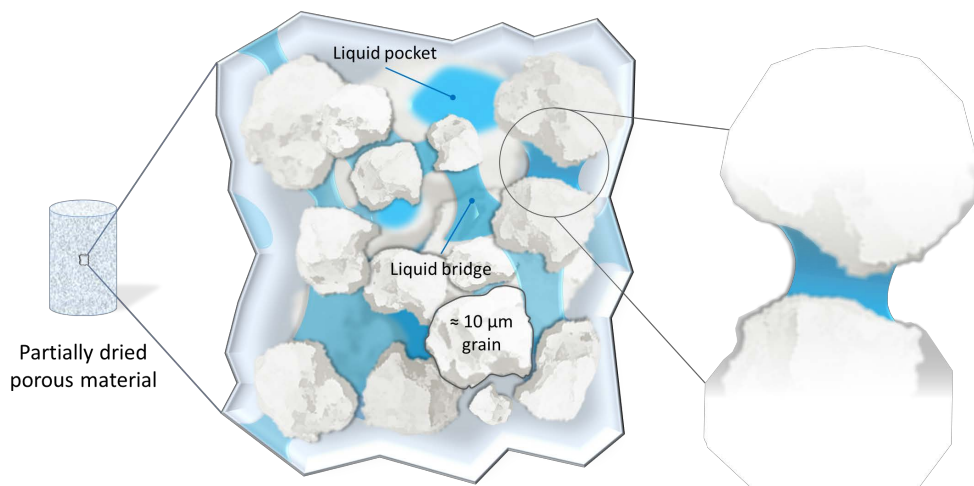


Figure 5. Schematic view of the microstructure of a porous material at the end of the drying process: the remaining liquid phase is in the form of isolated pockets or liquid bridges. The contact between the liquid and the substrate is crucial to the process.



Figure 6. Liquid bridge geometric parameters which have been investigated in the present study.

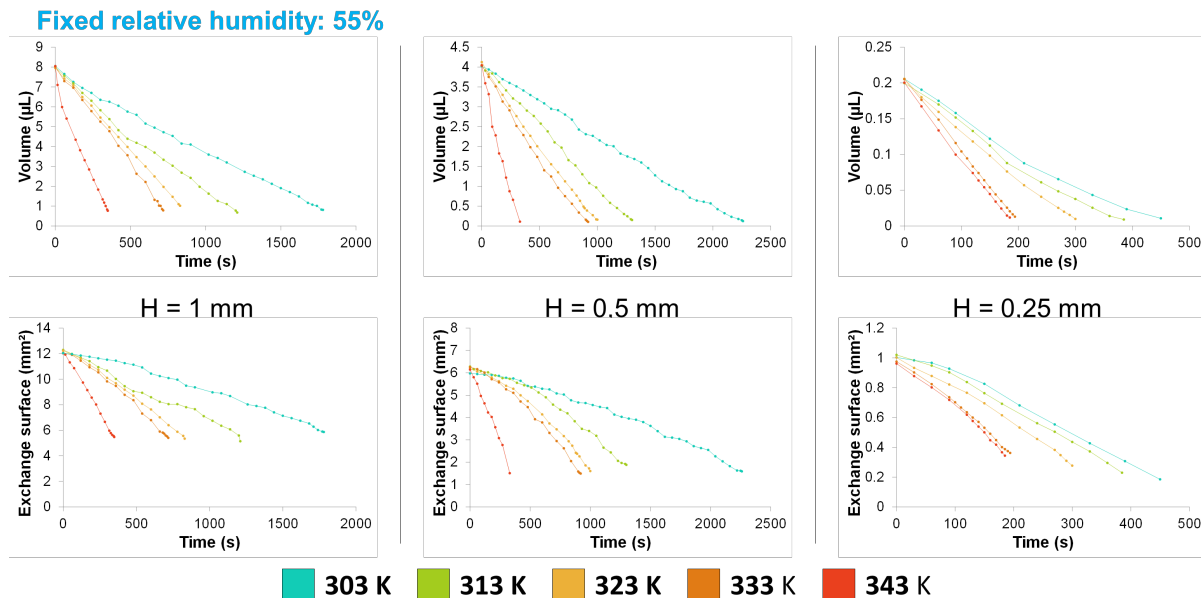


Figure 7. Evolution of the volume and exchange area of the liquid bridges as a function of time, from 303 K to 343 K at a fixed relative humidity of 55%.

Table 1. Liquid bridges height and their corresponding initial volume.

Liquid bridges height	1 mm	0.5 mm	0.25 mm
Corresponding initial volumes	8 μL	4 μL	0.2 μL

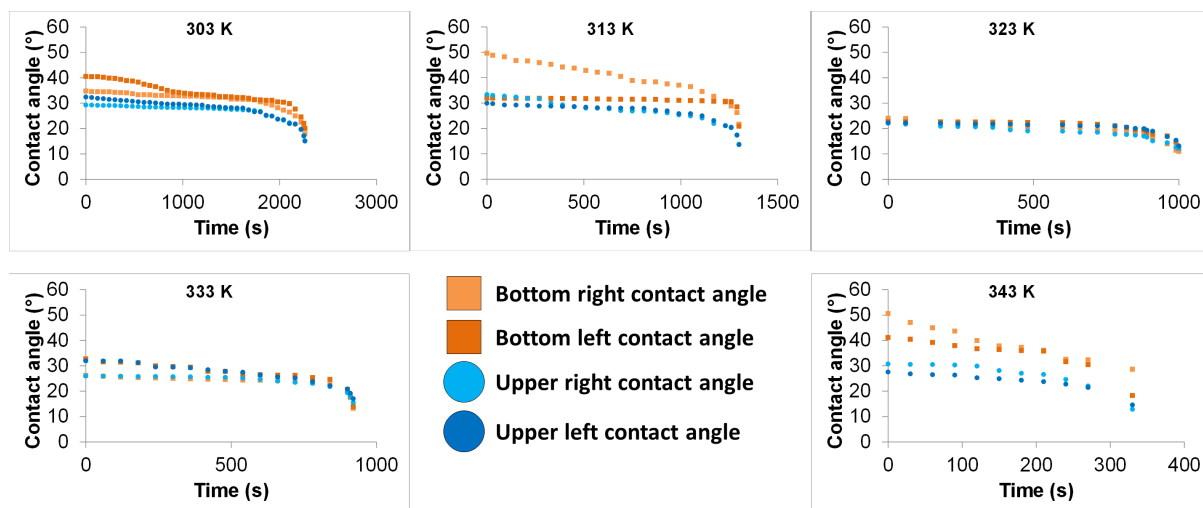


Figure 8. Evolution of the four contact angles of liquid bridges between two plates of silicon wafer, from 303 K up to 343 K at fixed relative humidity of 55% and a liquid bridge height of 0.5 mm.

Initial contact angles values are usually between 20° and 40° . Whatever the temperature is, the behavior is unchanged. In a first step, the contact angle slightly decreases, varying only of a few degrees. When the bridge is small enough and that the liquid shape becomes unstable, the evaporation induces a diminution of the neck radius of the liquid bridge, causing the contact angle to decrease drastically. It can be noted that one of the four initial contact angle is sometimes much higher than the others, thus revealing a pinning of the contact line around the observed region. Such an observation is illustrated **Figure 9** by the bottom left contact angle in the evolution of the liquid bridge at 313 K.

The pinned contact line reveals a local change of the surface state. Such type of simple observation could be related to the local rugosity of the substrate. It also should be noted that usually in the literature, only one of the four contact angles is considered when exploiting image analysis, whether it is liquid bridges between two plates or between two spheres [12]-[14].

3.3. Role of Relative Humidity

Erbil did notice a lack of relative humidity information in numerous recent papers when water evaporation was tackled [7]. Indeed, it can alter the evaporation rate. That is why the same measurements have been carried out at 323 K at relative humidities ranging from 35% up to 75%. Except for the drying kinetics, the relative humidity has no impact on the contact angles evolution. Results about volume and exchange surface are presented in **Figure 10**. Drying time is not significantly influenced at low relative humidity (35%, 45% and 55%). The drying time becomes much longer when reaching 65% and 75% relative humidity.

One suggestion that could be made from these observations is the following: in a porous ceramic material and after drying most of the network liquid, some pores are still filled with liquid. These pores emptying rate could be controlled by tuning the partial vapor pressure variations with time.

3.4. Liquid Bridge Break Observation

The rupture of a liquid bridge and the resulting deformations cannot be seen with the naked eye. This instability and the creation of two sessile droplets which last few tens of milliseconds were observed using a fast camera with a $15,000 \text{ images}\cdot\text{s}^{-1}$ frame rate. For these pictures, the liquid bridge height is set to 1 mm and the volume is less than $2 \mu\text{L}$. Images acquisitions are given in **Figure 11**. The liquid bridge is thinning more and more as the breaking approaches. The neck of the liquid bridge finally takes the shape of a cylinder before separating in two sessile drops (see the snap shot taken at 7.2 ms in **Figure 11**). When separating, a pinching can be observed on both sides. It is similar to that of a drop that detaches from a capillary tube by gravity which was previously observed in the literature [15].

This simple observation also underlines the phenomenon speed and intensity, where the capillary pressure

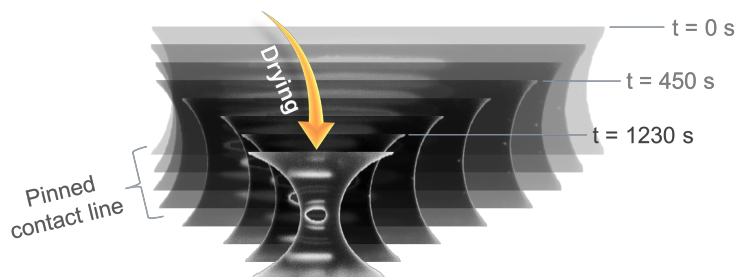


Figure 9. Illustration of the pinned contact line at the bottom left contact angle during drying a 0.5 mm height liquid bridge at 313 K.

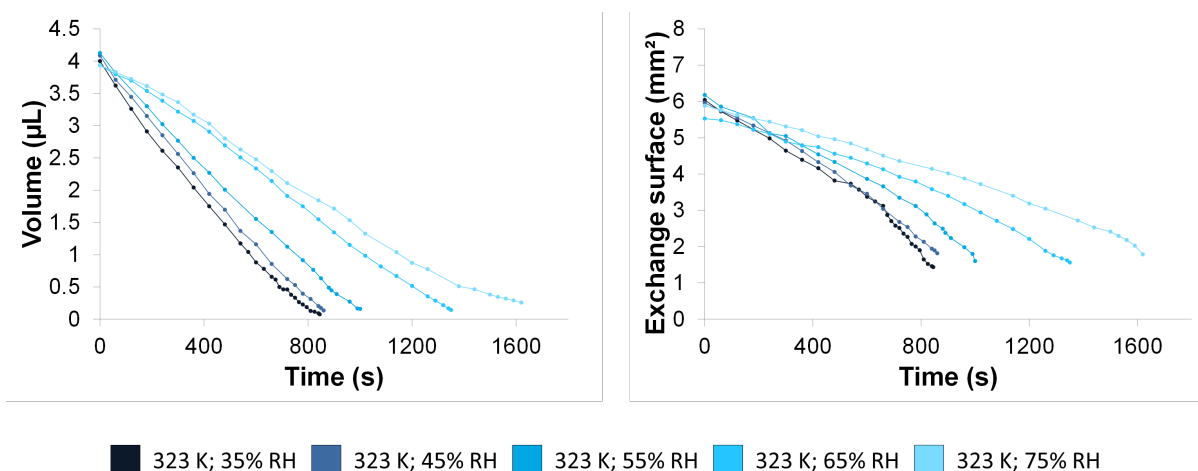


Figure 10. Evolution of the volume and exchange area of the liquid bridges as a function of time at 323 K, from 35% relative humidity up to 75% relative humidity.

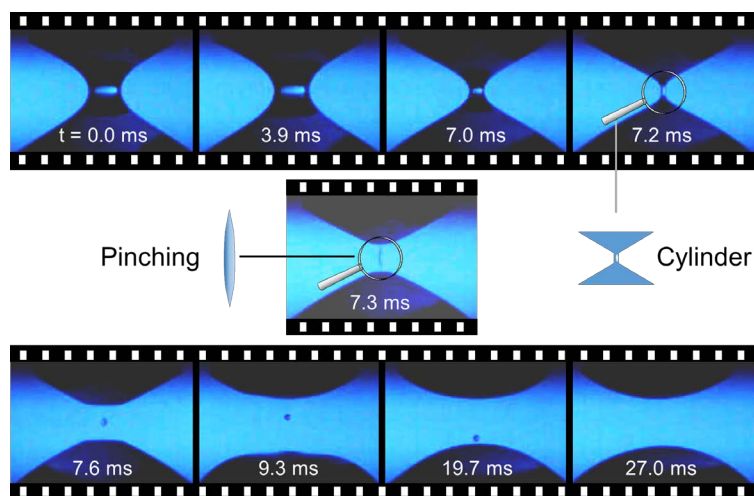


Figure 11. Breaking of a liquid bridge of 1 mm height: a cylindrical shape is observed before breaking (7.3 ms), where a pinching occurs on both sides, forming a droplet with a short life time.

within the liquid bridge vanishes in less than 10 milliseconds. Indeed this pressure (Laplace pressure) corresponds to a suction of the liquid. In the case of deionized water, the resulting capillary force mainly depends on the substrate surface [16] and the liquid volume. Instabilities have recently been underlined in the case of drying liquid bridges between two spheres, at the critical moment where the liquid breaks into two sessile drops [17]. This sudden release of pressure at the end of drying could be related to the swelling that is sometimes observed

in clay based materials and responsible for the formation of small cracks (research work in progress). From the initial setting time to $t = 7.3$ ms, the neck of the liquid bridge passes from a form of an unduloid to that of a cylinder. For these particular geometry changes, the interested reader may refer to recent literature which described the evolution of these unstable liquid forms [18] [19].

4. Research Interest and Future Work

The liquid bridges observation coupled with image analysis allowed evaluating their behavior during drying, at different temperatures and relative humidities. Drying kinetics has been studied. When trying to provide an accurate representation of the fluid behavior at a mesoscopic scale, we noticed a lack of effective data that prevented us from proposing models as close as possible to reality at usual drying temperatures and relative humidities. Recently, modeling methods allowed realistic representation of fluids, whether in the case of modeling a liquid in contact with a substrate or just the liquid behavior [20] [21]. However, there is still no general approach to reproduce all the effects due to the interaction between the liquid and the air or the substrate. That is why these new insights could lead to more accurate models. The interest is also to have a better picture of the phenomena occurring during drying at the liquid-substrate interface.

5. Conclusions

Using a specific device to create liquid bridges within a humid environment, values of geometrical parameters, namely the volume, the exchange surface and contact angles of liquid bridges as a function of the drying time have been evaluated for temperatures from 303 to 343 K and relative humidities from 35% to 75%. Drying time decreases when temperature increases and relative humidity decreases. The measurement of the four contact angles at a given time reveals that they don't always follow the same trend, due to different substrate surface states. Thus, the choice of the contact angle, which is necessary to obtain an estimated value of the Laplace pressure by image analysis, should be mentioned when dealing with evaporating liquid bridges.

The break of a liquid bridge at the end of drying has been observed with a high speed camera and revealed that the time interval in which the capillary pressure and the adhesion force are released is about tens of milliseconds. Consequently, cracks formation observed at the end of the drying stage of a porous material can be linked to such phenomenon. Finally, we intend that the proposed study can provide new data for a predictive microscopic model close to real cases, such as the behavior of water within a porous material subjected to different temperatures and relative humidities.

Acknowledgements

The authors gratefully acknowledge the financial support provided by the Limousin region as part of the PhD of Etienne Portuguez.

References

- [1] Boch, P. and Niepce, J.-C. (2010) *Ceramic Materials, Properties, and Applications*. John Wiley & Sons Ltd., Hoboken.
- [2] Scherer, G.W. (1990) Theory of Drying. *Journal of the American Ceramic Society*, **73**, 3-14. <http://dx.doi.org/10.1111/j.1151-2916.1990.tb05082.x>
- [3] Jouenne, C.A. (1975) *Traité de céramiques et matériaux minéraux*. Editions Septima.
- [4] Whitaker, S. (1986) Flow in Porous Media I: A Theoretical Derivation of Darcy's Law. *Transport in Porous Media*, **1**, 3-25. <http://dx.doi.org/10.1007/BF01036523>
- [5] Nadeau, J.P. and Puiggali, J.R. (1995) *Drying: Physical Processes to Industrial Processes*. Lavoisier, Paris.
- [6] deGennes, P.-G., Brochard-Wyart, F. and Quéré, D. (2004) *Capillarity and Wetting Phenomena-Drops, Bubbles, Pearls, Waves*. Springer-Verlag, New York. <http://dx.doi.org/10.1007/978-0-387-21656-0>
- [7] Erbil, H.Y. (2006) *Surface Chemistry of Solid and Liquid Interfaces*. Blackwell Publishing, Oxford.
- [8] Pérez-Díaz, J.L., Álvarez-Valenzuela, M.A. and García-Prada, J.C. (2012) The Effect of the Partial Pressure of Water Vapor on the Surface Tension of the Liquid Water-Air Interface. *Journal of Colloid and Interface Science*, **381**, 180-182. <http://dx.doi.org/10.1016/j.jcis.2012.05.034>
- [9] Portuguez, E., Alzina, A., Michaud, P., Oudjedi, M. and Smith, A. (2016) Evolution of a Water Pendant Drop: Effect

of Temperature and Relative Humidity. (Unpublished)

- [10] Mielniczuk, B., Hueckel, T. and El Youssoufi, M.S. (2014) Evaporation-Induced Evolution of the Capillary Force between Two Grains. *Granular Matter*, **16**, 815-828. <http://dx.doi.org/10.1007/s10035-014-0512-6>
- [11] Bormashenko, E.Y. (2013) Wetting of Real Surfaces. Walter de Gruyter, Berlin. <http://dx.doi.org/10.1515/9783110258790>
- [12] Rabinovich, Y.I., Esayanur, M.S. and Moudgil, B.M. (2005) Capillary Forces between Two Spheres with a Fixed Volume Liquid Bridge: Theory and Experiment. *Langmuir*, **21**, 10992-10997. <http://dx.doi.org/10.1021/la0517639>
- [13] Zhou, Z., Li, Q. and Zhao, X.S. (2006) Evolution of Interparticle Capillary Forces during Drying of Colloidal Crystals. *Langmuir*, **22**, 3692-3697. <http://dx.doi.org/10.1021/la052934c>
- [14] Chen, H., Amirfazli, A. and Tang, T. (2013) Modeling Liquid Bridge between Surfaces with Contact Angle Hysteresis. *Langmuir*, **29**, 3310-3319. <http://dx.doi.org/10.1021/la304870h>
- [15] Shi, X.D., Brenner, M.P. and Nagel, S.R. (1994) A Cascade of Structure in a Drop Falling from a Faucet. Science, New York, Washington DC, 219-219. <http://dx.doi.org/10.1126/science.265.5169.219>
- [16] Butt, H.J. (2008) Capillary Forces: Influence of Roughness and Heterogeneity. *Langmuir*, **24**, 4715-4721. <http://dx.doi.org/10.1021/la703640f>
- [17] Mielniczuk, B., Hueckel, T. and El Youssoufi, M.S. (2015) Laplace Pressure Evolution and Four Instabilities in Evaporating Two-Grain Liquid Bridges. *Powder Technology*, **283**, 137-151. <http://dx.doi.org/10.1016/j.powtec.2015.05.024>
- [18] Gagneux, G. and Millet, O. (2014) Analytic Calculation of Capillary Bridge Properties Deduced as an Inverse Problem from Experimental Data. *Transport in Porous Media*, **105**, 117-139. <http://dx.doi.org/10.1007/s11242-014-0363-y>
- [19] Langbein, D.W. (2002) Capillary Surfaces: Shape—Stability—Dynamics, in Particular under Weightlessness. Springer, Berlin. <http://dx.doi.org/10.1007/3-540-45267-2>
- [20] Tartakovsky, A. and Meakin, P. (2005) Modeling of Surface Tension and Contact Angles with Smoothed Particle Hydrodynamics. *Physical Review E*, **72**, 206301. <http://dx.doi.org/10.1103/PhysRevE.72.026301>
- [21] Akinci, N., Akinci, G. and Teschner, M. (2013) Versatile Surface Tension and Adhesion for SPH Fluids. *ACM Transactions on Graphics*, **32**, Article No. 182. <http://dx.doi.org/10.1145/2508363.2508395>



Scientific Research Publishing

Submit or recommend next manuscript to SCIRP and we will provide best service for you:

Accepting pre-submission inquiries through Email, Facebook, LinkedIn, Twitter, etc
A wide selection of journals (inclusive of 9 subjects, more than 200 journals)
Providing a 24-hour high-quality service
User-friendly online submission system
Fair and swift peer-review system
Efficient typesetting and proofreading procedure
Display of the result of downloads and visits, as well as the number of cited articles
Maximum dissemination of your research work

Submit your manuscript at: <http://papersubmission.scirp.org/>